THE JOURNAL OF BIOLOGICAL CHEMISTRY VOL. 287, NO. 22, pp. 18103–18114, May 25, 2012


# *N*-Methyl-D-aspartate (NMDA) Receptor Composition Modulates Dendritic Spine Morphology in Striatal Medium Spiny Neurons*

Received for publication, January 28, 2012, and in revised form, April 2, 2012 Published, JBC Papers in Press, April 9, 2012, DOI 10.1074/jbc.M112.347427

**Csaba Vastagh[‡1,2], Fabrizio Gardoni[‡1,3], Vincenza Bagetta[§], Jennifer Stanic[‡], Elisa Zianni[‡], Carmen Giampà[§], Barbara Picconi[§], Paolo Calabresi[§¶], and Monica Di Luca[‡]**

*From the [‡]Department of Pharmacological Sciences, University of Milano, Via Balzaretti 9, 20133 Milano, Italy, [§]Laboratorio di Neurofisiologia, Fondazione Santa Lucia, Istituto di Ricovero e Cura a Carattere Scientifico, 00143 Rome, Italy, and [¶]Clinica Neurologica, Università di Perugia, Ospedale S. Maria della Misericordia, 06156 Perugia, Italy*

**Background:** An interplay between dopamine (DA) and NMDA receptors in striatum is essential to drive motor behavior.
**Results:** NR2A antagonist induces an increase of spine head width as induced by D1 activation.
**Conclusion:** NMDA receptor subunit composition regulates dendritic spine morphology in MSNs.
**Significance:** Therapies targeted to modulate NMDA receptor subunits may lead to a morphological outcome in dendritic spines of MSNs.

**Dendritic spines of medium spiny neurons represent an essential site of information processing between NMDA and dopamine receptors in striatum. Even if activation of NMDA receptors in the striatum has important implications for synaptic plasticity and disease states, the contribution of specific NMDA receptor subunits still remains to be elucidated. Here, we show that treatment of corticostriatal slices with NR2A antagonist NVP-AAM077 or with NR2A blocking peptide induces a significant increase of spine head width. Sustained treatment with D1 receptor agonist (SKF38393) leads to a significant decrease of NR2A-containing NMDA receptors and to a concomitant increase of spine head width. Interestingly, co-treatment of corticostriatal slices with NR2A antagonist (NVP-AAM077) and D1 receptor agonist augmented the increase of dendritic spine head width as obtained with SKF38393. Conversely, NR2B antagonist (ifenprodil) blocked any morphological effect induced by D1 activation. These results indicate that alteration of NMDA receptor composition at the corticostriatal synapse contributes not only to the clinical features of disease states such as experimental parkinsonism but leads also to a functional and morphological outcome in dendritic spines of medium spiny neurons.**

Activation of NMDA receptors represents a crucial step for long lasting changes in the strength of excitatory synaptic transmission and plays a major role in the rearrangement of synaptic circuits (1, 2). In hippocampus, synaptic NMDA receptors are involved in the induction of long term potentiation, which entails a long lasting increase in excitatory post-synaptic transmission and modification of dendritic spine morphology (3, 4). In contrast, chronic blockade with NMDA receptor antagonists on mature spines results in no significant change in spine density, although many long (2 $\mu$m) thin dendritic protrusions resembling filopodia are formed as a consequence (5, 6).

In the striatum, glutamatergic cortical afferents converge with dopaminergic terminals from the substantia nigra pars compacta onto the dendritic spines of medium spiny neurons (MSNs).[4] In particular, dopaminergic terminals form synaptic contacts in the neck of MSNs spines, whereas the head of the spine receives inputs from glutamatergic terminals (7). Consequently, dendritic spines of striatal MSNs are an essential site of information processing between glutamate and dopamine both in physiological conditions and in neurodegenerative events, *i.e.* in Parkinson disease (PD) (8). In addition, several studies described the co-localization of D1 and NMDA receptors in the MSN dendritic spine, indicating the existence of a direct molecular interaction and a functional cross-talk between the two receptor signaling pathways (9–11).

It has been demonstrated clearly that all MSNs express both NR2A and NR2B subunits of the NMDA receptor (12). In particular, some studies demonstrated the presence of heterotrimeric NR1/NR2A/NR2B receptor assemblies (13), whereas pure NR1/NR2A and NR1/NR2B heterodimeric assemblies are only partially involved in synaptic transmission (14). Interestingly, heterotrimeric NR1/NR2A/NR2B assemblies predominate at striatal MSN synapses (15).

Notably, NMDA receptors in corticostriatal synapse show a peculiar behavior as it has been proposed that NR2A containing

* This work was supported by European Community FP7 Contracts 222918 (REPLACES; to P. C. and M. D. L.), 217902 (cPADS; to M. D. L.), and 238608 (Symbad (to M. D. L.); Progetto Strategico 2007 (to P. C., B. P., and M. D. L.); Progetto Giovani Ministero Sanità 2008 (to B. P. and F. G.); and Cariplo Foundation Project 2010-0661 (to F. G. and B. P.).
[1] Both authors contributed equally to this work.
[2] Present address: Laboratory of Endocrine Neurobiology, Inst. of Experimental Medicine of the Hungarian Academy of Sciences, Szigony u. 43, Budapest H-1083, Hungary.
[3] To whom correspondence should be addressed: Dept. of Pharmacological Sciences, University of Milano, Via Balzaretti 9, 20133 Milan, Italy. Tel.: 39-0250318374; E-mail: fabrizio.gardoni@unimi.it.

[4] The abbreviations used are: MSN, medium spiny neuron; PD, Parkinson disease; PSD, postsynaptic density; Ab, antibody; TIF, Triton-insoluble postsynaptic fraction; EGFP, enhanced GFP; SP, substance P; EPSC, excitatory postsynaptic current; AMPAR, AMPA receptor; NMDAR, NMDA receptor; $BS^3$, *bis*-(sulfosuccinimidyl)-suberate; CNQX, 6-cyano-7-nitroquinoxaline-2,3-dione.

but not NR2B containing NMDA receptors regulates the homeostasis of corticostriatal transmission (16), although NR2B is the predominant NR2 subunit expressed in the striatum (17). In addition, recent reports have suggested that NR2A and NR2B subunits differentially sculpt glutamatergic inputs in striatal MSNs (10); pharmacological blockade of NR2A and NR2B subunits affects the amplitude and kinetics of NMDA responses and produces contrasting effects on D1 receptor modulation (10).

In this context, even if it is known that alterations of NMDA receptor composition at the corticostriatal synapse contribute to the clinical features of disease states, *i.e.* PD and Huntington disease (18–20), the possible functional and morphological outcome of NMDA receptor subunit composition in dendritic spines of MSNs still remains unclear.

Here, we show that modulation of the levels of NR2A-containing NMDA receptors at synaptic sites is *per se* sufficient to induce a significant alteration of dendritic spine morphology at MSN levels. Treatment with NR2A antagonist or with NR2A blocking peptide induces morphological modifications of dendritic spines as induced by D1 receptor activation.

## EXPERIMENTAL PROCEDURES

*Antibodies, Reagents, and Cell-permeable Peptides*—The following antibodies (Ab) were used: mAb anti-tubulin from Sigma-Aldrich; polyclonal Ab anti-D1 from Abcam; polyclonal Ab anti-NR2B and mAb anti-NR2A from Zymed Laboratories Inc.; polyclonal Ab anti-GluR1 and mAb anti-GluR2 from Millipore; mAb anti-PSD-95 from Neuromab, mAb NR1 from Invitrogen. NVP-AAM0077 was provided kindly by Novartis. AP-5, CNQX, ifenprodil hemitartrate, and picrotoxin were provided by Tocris Cookson. Cell-permeable peptides were obtained linking the 11 amino acids (YGRKKRRQRRR) human immunodeficiency virus TAT transporter sequence to the last C-terminal nine amino acids of NR2A (TAT2A) or to the last nine amino acids of NR2B (TAT2B) (21, 22). TAT2A(-SDV) or TAT2B(-SDV) inactive peptides (lacking the last C-terminal three amino acids of NR2A or NR2B) were used as negative controls. All peptides were synthesized by Xigen Pharma. For *in vitro* electrophysiological recordings, drugs were applied by diluting them in Kreb's solution to the final concentration and by switching the perfusion from control to drug-containing solution.

*Corticostriatal Slices*—Adult (8-week-old) male Wistar rats were decapitated, and brains were removed quickly from the skulls. Consecutive series of corticostriatal slices were cut at 270-$\mu$m thickness using a vibratome. Slices were then placed into custom-made chambers filled with Kreb's buffer (124 mM NaCl, 3.3 mM KCl, 1.2 mM $KH_2PO_4$, 1.3 mM $MgSO_4$, 2.5 mM $CaCl_2$, 20 mM $NaHCO_3$, and 10.0 mM glucose) equilibrated continuously with $O_2$ (95%) and $CO_2$ (5%). After the preincubation period (1 h), slices were treated with the different compounds (45 min) as indicated under "Results." Control series of slices were maintained in the vehicle alone. Striatal areas were carefully isolated and collected on dry ice for further processing.

*In Vivo Treatments*—For *in vivo* experiments, adult (8-week-old) male Wistar rats were injected (i.p.) with SKF38393 (2 mg/ml/kg) in the presence or absence of NVP-AAM077 (2 mg/kg) or ifenprodil (20 mg/kg), or vehicle only. 45 min later, animals were sacrificed, and whole striata were collected and snap-frozen on dry ice immediately. Samples were kept deep-frozen until further processing. All experiments were carried out according to the guidelines on the ethical use of animals from the European Communities Council Directive of 24 November 1986 (86/609/EEC).

*Preparation of TIF Fractions*—A Triton-insoluble postsynaptic fraction (TIF) was purified from striatal tissue using a previously validated biochemical fractionating method (22, 23). Briefly, whole striatal tissue was homogenized in 0.32 M ice-cold sucrose, containing 1 mM Hepes, 1 mM $MgCl_2$, 1 mM EDTA, 1 mM $NaHCO_3$, 0.1 mM PMSF at pH 7.4 in presence of a complete set of protease inhibitors (Complete™, Roche Diagnostics) and phosphatase inhibitors (Sigma-Aldrich). The homogenized tissue was centrifuged at 1000 × *g* for 10 min at 4 °C. The resulting supernatant (S1) was centrifuged at 13,000 × *g* for 15 min to obtain a crude membrane fraction (P2 fraction). The pellet was resuspended in 1 mM Hepes + Complete™ in a glass-glass Potter-Elvehjem tissue grinder and centrifuged at 100,000 × *g* for 1 h. The pellet (P3) was resuspended in buffer containing 75 mM KCl and 1% Triton X-100 and centrifuged at 100,000 × *g* for 1 h. The final pellet (P4) was homogenized in a glass-glass Potter-Elvehjem tissue grinder in 20 mM Hepes. Then, an equal volume of glycerol was added and this fraction, referred to as the TIF, was stored at −80 °C until processing. TIF fraction was used instead of the classical postsynaptic density (PSD) because of the limited amount of starting material. Protein composition of this preparation was tested for the absence of presynaptic synaptic vesicle marker synaptophysin and the high enrichment in the PSD proteins (23).

*Surface Expression Assay*—Cross-linking experiments by means of the membrane-impermeable reagent *bis*-(sulfosuccinimidyl)-suberate ($BS^3$) were performed as described previously (24) to evaluate the AMPA and NMDA receptor subunit intracellular pool. Free-floating sections were shaken gently in the presence or absence of $BS^3$ solution (1 mg/ml in PBS) for 30 min at room temperature. Excess of $BS^3$ were removed by repeated washes in presence of ethanolamine; striatal areas were separated from cortex and homogenized in a glass-glass Potter-Elvehjem tissue grinder. The AMPA and NMDA subunit surface pool was not detectable following treatment of slices with $BS^3$ because of the formation of high-molecular weight aggregates that did not enter the gel.

*Immunoprecipitation*—50 $\mu$g of homogenate was incubated in a buffer containing 200 mM NaCl, 10 mM EDTA, 10 mM $Na_2HPO_4$, 0.5% Nonidet P-40, and 0.1% SDS with antibody against D1 receptor overnight at 4 °C. Protein A-Sepharose beads (Sigma-Aldrich) were added, and incubation was continued for 2 h at room temperature with shaking. Beads were collected by centrifugation at 1000 × *g* for 5 min and washed three times before adding sample buffer for SDS-PAGE and boiling for 5 min. Beads were collected by centrifugation, and all supernatants were applied onto 6% SDS-PAGE.

*Western Blotting*—Western blotting analysis was performed as described before with minor modifications (22). Samples (10 $\mu$g) were applied to SDS-PAGE and electroblotted. For each homogenate and TIF preparation, three independent Western

blotting experiments were run. Quantification of Western blot analysis was performed by means of computer-assisted imaging (ImageJ) after normalization on tubulin levels.

*Immunofluorescence Labeling*— drd1-EGFP and drd2-EGFP bacterial artificial chromosome (BAC) transgenic mice were deeply anesthetized and perfused with PBS followed by 4% paraformaldehyde in 0.1 M PB containing 0.2% picric acid and 0.02% glutaraldehyde. Brains were removed from the skulls and were postfixed overnight at 4 °C in the same fixative omitting glutaraldahyde. Sections were cut with a vibratome in the sagittal plane at a 40-$\mu$m thickness. Free-floating sections were then washed in PBS several times, pretreated with 0.5% Triton X-100 for 30 min, and incubated in 4% horse serum/1% BSA for 1.5 h. Primary antibodies (NR2A and NR2B, 1:500; GFP, 1:1000) were applied overnight at 4C, diluted in 4% horse serum/PBS. Secondary antibodies (Alexa Fluor 488 goat anti-mouse, Alexa Fluor 555 goat anti-rat, Alexa Fluor goat anti-rabbit 633; Invitrogen, 1:2000) were applied for 2 h at room temperature. Immunoreacted sections were mounted and coverslipped. Acquisition of fluorescent images were performed with a Zeiss LSM 510 confocal microscope.

*Substance-P Immunohistochemistry, Spine Morphology, and Data Analysis*—Combination of immunohistochemistry with diolistic labeling was performed as described previously with minor modifications (25). Direct pathway MSNs were immunohistochemically identified as "substance P-positive" ($SP^+$). Briefly, animals were deeply anesthetized and perfused with 0.1 M PB followed by 1.5% paraformaldehyde in 0.1 M PB. Brains were sectioned with a vibratome in the coronal plane at 40-$\mu$m thickness. Sections containing striatal areas were selected for diolistic labeling. Tungsten particles and tubes were prepared according to the manufacturer's instructions. DiI-coated particles were delivered onto corticostriatal slices with a handheld gene gun (Helios, Bio-Rad) at a pressure of 1.6–1.8 psi. DiI-labeled sections were stored in 0.04% paraformaldehyde overnight at 4 °C. On the next day, permeabilization (0.05% Triton X-100 for 15 min) and blocking step (5% normal horse serum) were followed by incubation with anti-substance P primary antibody (Millipore, 1:300) for 36 h at 4 °C. Secondary Ab (Alexa Fluor 488, 1:500) were used overnight at 4 °C. Sections were then mounted, covered in Permafluor (Sigma-Aldrich), and analyzed on a Zeiss LSM-510 laser confocal microscope. Confocal z-stacks of double-stained MSN neurons were acquired with a 63× objective at 0.5-$\mu$m intervals, and a projection image was rendered. At least 10 z-stack images were acquired for each animal and for each area of interest. Analysis of dendritic spine morphology was performed with ImageJ software; for each dendritic spine, length and head width were measured, which have been used to classify dendritic spines into categories (26). In particular, protrusions having the length longer than 3 $\mu$m were considered filopodia, and the others were considered spines.

*Whole-cell Recordings*—Coronal corticostriatal brain slices (240–270-$\mu$m thickness) were transferred to a submerged recording chamber, perfused (2–3 ml/min) with oxygenated artificial cerebrospinal fluid, and visualized with 20× and 40× water immersion objectives (Nikon) using standard infrared and differential interference contrast microscopy. Whole-cell recordings were performed using 1.5-mm external diameter borosilicate pipettes. For the voltage-clamp recordings, electrodes (3.5–5 megohms) were filled with a solution containing the following: 120 mM $CsMeSO_3$, 15 mM CsCl, 8 mM NaCl, 0.2 mM EGTA, 10 mM Hepes, 2 mM Mg-ATP, 0.3 mM Na-GTP, 10 mM tetraethylammonium, and 5 mM QX-314, adjusted to pH 7.2 with CsOH.

*Analysis of NMDA/AMPA Receptor Ratio*—Neurons were voltage clamped at −70 mV and +40 mV to record, respectively, AMPA receptor- and NMDA receptor-mediated excitatory postsynaptic currents (EPSCs). A bipolar stimulating electrode was placed 100–300 $\mu$m rostral to the recording electrode and used to stimulate excitatory terminals at 0.1 Hz. NMDA EPSCs were pharmacologically isolated at +40 mV by the application of the AMPA antagonist CNQX (10 $\mu$M), whereas the NMDA receptor-NR2A component was obtained by applying ifenprodil 3–10 $\mu$M after a stable recording of the NMDA component. The NMDA/AMPA receptor ratio was calculated by dividing the peak NMDA receptor-mediated EPSCs by the AMPA receptor-mediated EPSCs. Similarly, the NMDA-NR2A/AMPA receptor ratio was calculated by dividing NMDA-NR2A-mediated EPSCs by the AMPA receptor-mediated EPSCs. Recordings in whole-cell patch clamp were made using MultiClamp 700 B (Molecular Devices) and were acquired at 10 kHz using pClamp10 software (Axon Instrument) and a data acquisition unit (Digidata 1440A; Molecular Devices). Input resistances and injected currents were monitored throughout the experiments. Variations of these parameters >20% led to the rejection of the experiment.

For spontaneous excitatory postsynaptic currents, MSNs were clamped at the holding potential ($V_h$) of −70 mV. Data were acquired with pClamp (version 10.2); current was filtered at 0.1 kHz and digitized at 200 $\mu$s using Clampex (gap-free mode; version 10.2) and analyzed offline using the automatic detection and subsequently checked manually for accuracy. The threshold amplitude for the detection of an event (5 pA) was adjusted above root mean square noise level (2–3 pA at $V_h = -70$ mV). For the experiments on NMDA-isolated currents, neurons were clamped at +40 mV, incubated with picrotoxin and CNQX until a stable recording was obtained and SKF38393 was bath-applied for 45 min.

## RESULTS

*NR2A but Not NR2B Antagonist Modulates Dendritic Spine Morphology in MSNs*—Corticostriatal slices were incubated with selective antagonists of NR2A-containing *versus* NR2B-containing NMDA receptors (respectively, NVP-AAM077 and ifenprodil). As shown in Fig. 1*A*, application of NR2A antagonist (NVP-AAM077; 300 nM; 45 min), progressively and significantly reduced the amplitude of the NMDA-isolated currents to 36.42 ± 5.1% of the control ($n = 4$; **, $p < 0.01$). Similarly, treatment of the corticostriatal slices with ifenprodil (10 $\mu$M; 45 min), a known antagonist of the NR2B subunit, reduced the amplitude of the NMDA evoked current to 41.51 ± 6.49% of control ($n = 6$; ***, $p < 0.001$) (Fig. 1*A*). Treatment either with NVP-AAM077 or with ifenprodil did not induce any modification of NR2A or NR2B subunit levels in a TIF ($n = 4$; $p > 0.05$; Fig. 1*B*). Furthermore, no alteration of D1 receptor localization in the

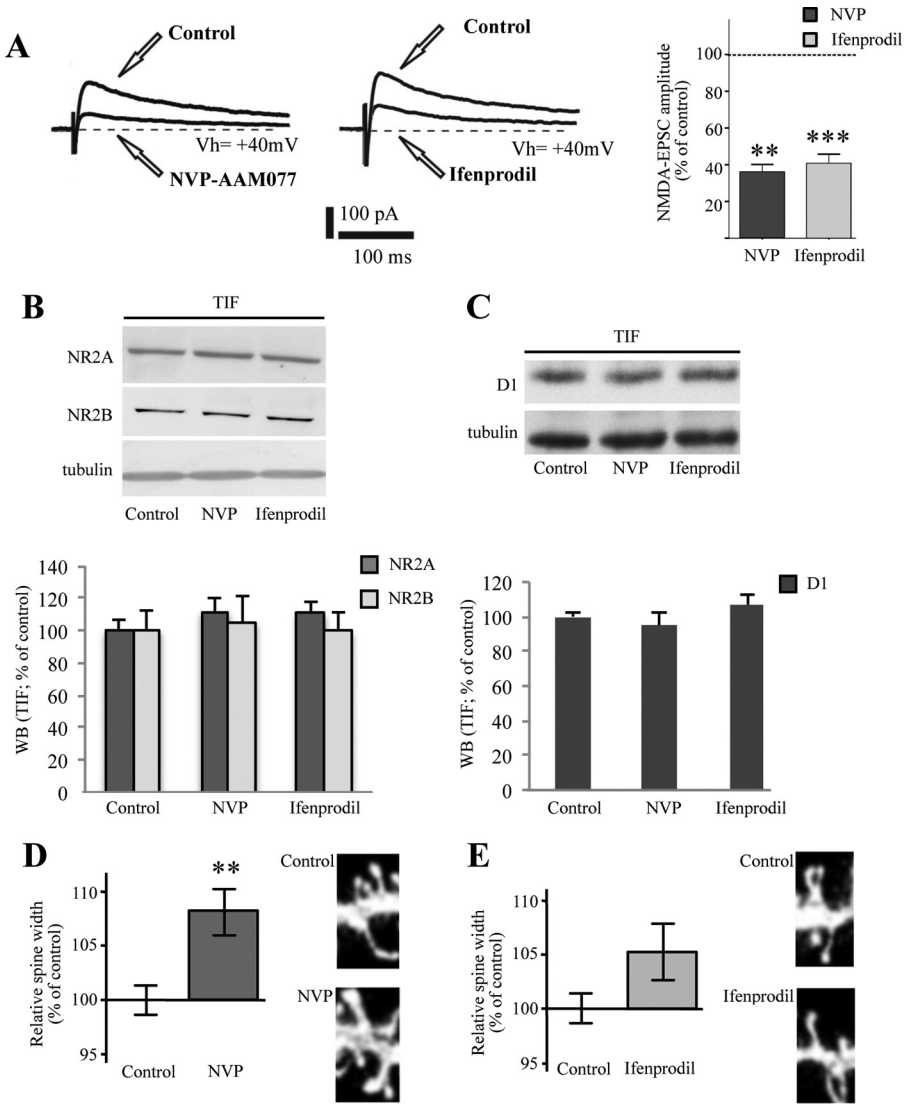


FIGURE 1. **Effect of NR2A and NR2B antagonists on dendritic spine morphology in MSNs.** *A*, *left panel*: sample traces of the NMDA isolated currents at +40 mV before and after bath application of the NR2A selective antagonist NVP-AAM077 (300 nM). *Right panel*: sample traces of the NMDA-isolated currents (+40 mV) before and after the application of the NR2B subunit antagonist ifenprodil (10 $\mu$M). Shown is a bar graph showing the effects of NVP-AAM077 300 nM (*t* test; **, $p < 0.01$, pre- *versus* post-application 36.42 ± 5.1%; $n = 4$) and ifenprodil (*t* test; ***, $p < 0.001$, pre- *versus* post-application, 41.51 ± 6.49%; $n = 6$) on the NMDA-EPSC amplitude. *B*, Western blot analysis of NR2A and NR2B subunits and tubulin performed from the TIF obtained from control, NVP-AAM077 (*NVP*, 300 nM) and ifenprodil-treated (10 $\mu$M) corticostriatal slices. The same amount of proteins was loaded in each lane. The graph displays the results of Western blot analysis expressed as control percentage. *C*, Western blot analysis of D1 receptor and tubulin performed from TIF obtained from control, NVP-AAM077 (*NVP*, 300 nM) and ifenprodil-treated (10 $\mu$M) corticostriatal slices. The same amount of proteins was loaded in each lane. The graph displays the results of Western blot analysis expressed as control percentage. *D*, diagram showing relative average spines head width (*t* test; **, $p < 0.005$, NVP-AAM077 *versus* control; $n > 500$ spines from 10 different neurons for each group) of MSNs from control or NVP-AAM077-treated rats. Representative images show dendrites of medium spiny neurons from control or NVP-AAM077-treated corticostriatal slices. *E*, diagram showing relative average spines head width of medium spiny neurons from control or ifenprodil-treated corticostriatal slices (*t* test; $p > 0.05$, ifenprodil *versus* control, $n > 500$ spines from 10 different neurons for each group). Representative images show dendrites of MSNs from control or ifenprodil-treated corticostriatal slices.

postsynaptic compartment was observed following treatment with NVP-AAM077 or ifenprodil (Fig. 1*C*; $n = 4$; $p > 0.05$).

As shown in Fig. 1*E*, no significant change in dendritic spine head width was observed after treatment with ifenprodil ($p > 0.05$, ifenprodil *versus* control). Conversely, statistical analysis revealed a significant increase in spine head width after treatment with NVP-AAM077 (**, $p < 0.005$, NVP-AAM007 *versus* control; Fig. 1*D*). No changes in the mean spine density were found after treatment with ifenprodil or NVP-AAM077 (data not shown).

*Modulation of NR2A/NR2B Ratio at Synaptic Sites Modulates Dendritic Spine Morphology*—It is well established that interactions of NR2A and NR2B subunits C-terminal regions with PDZ domains of PSD-MAGUK proteins play an important role in the regulation of NMDA receptors localization at synaptic sites (22, 27). Previous reports showed that cell-permeable peptides, corresponding to the last nine amino acids of the NR2A or NR2B protein fused to the TAT sequence (namely TAT2A or TA2B), reduce NR2A or NR2B binding to PSD-MAGUKs and induce a consequent decrease in the synaptic levels of NR2A- or NR2B-containing NMDA receptors (18, 21, 28). Corticostriatal slices were incubated with TAT2A or TAT2B peptides to test the role of NR2A or NR2B synaptic localization on dendritic spine morphology in MSNs. Treatment with TAT2A(-SDV) or TAT2B(-SDV) peptides (lacking

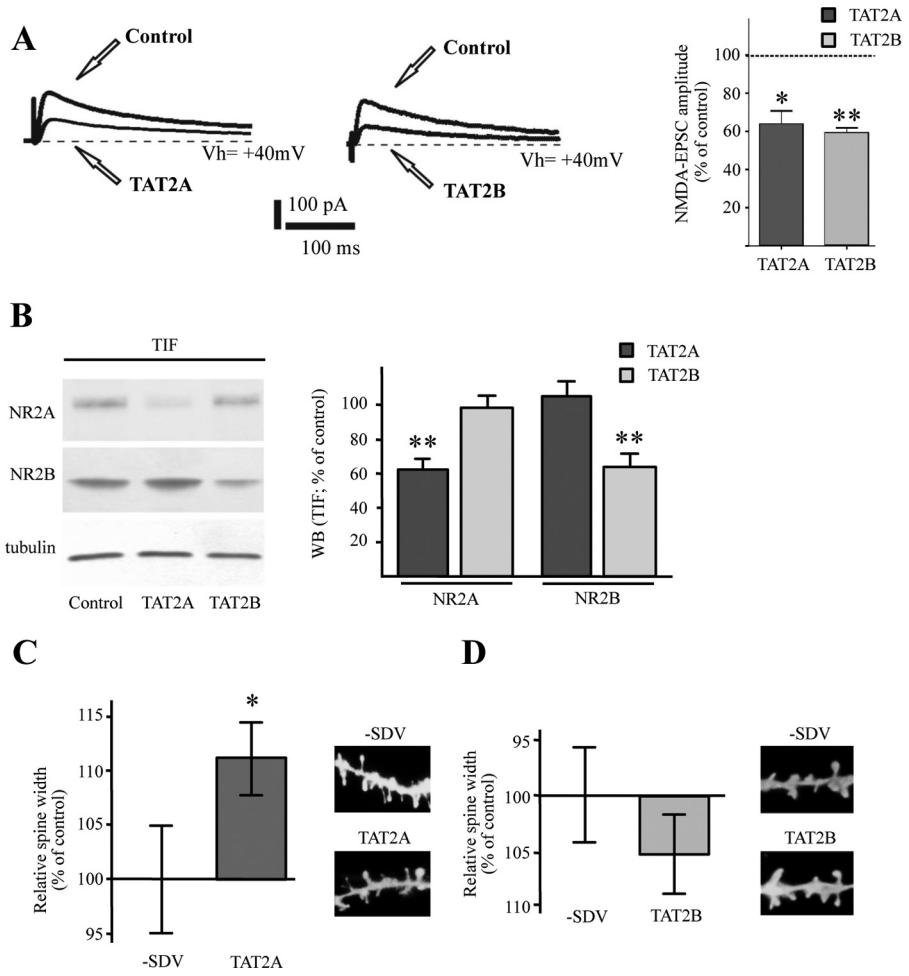


FIGURE 2. **Effect of the selective NR2A and NR2B uncoupling peptides on dendritic spine morphology of MSNs.** *A*, sample traces of the effect of the NR2A selective uncoupling peptide TAT2A and TAT2B on the NMDA isolated currents evoked at +40 mV and bar graph showing the percentage of the NMDA-EPSC amplitude that is blocked by the drugs, respectively, TAT2A (*right panel*; *t* test; *, $p < 0.05$, pre- *versus* post-TAT2A application, 64.03 ± 8.81%; $n = 4$) and TAT2B (*right panel*; *t* test; **, $p < 0.01$, pre- *versus* post-application, 59.83 ± 2.62%; $n = 4$). *B*, Western blot analysis of NR2A and NR2B subunits performed from the TIF obtained from control, TAT2A-treated (300 nM) or TAT2B-treated (300 nM) corticostriatal slices. The same amount of proteins was loaded in each lane. The graph displays the results of Western blot analysis expressed as control percentage (*t* test; **, $p < 0.01$). *C*, diagram showing relative average spines head width (*t* test; *, $p < 0.05$; TAT2A *versus* TAT2A(-SDV); $n > 500$ spines from 10 different neurons for each group) of MSNs from TAT2A and TAT2A(-SDV)-treated rats. Representative images show dendrites of medium spiny neurons from TAT2A and TAT2A(-SDV)-treated rats. *D*, diagram showing relative average spines head width of medium spiny neurons from TAT2B and TAT2B(-SDV)-treated rats (*t* test; $n > 500$ spines from 10 different neurons for each group). Representative images show dendrites of medium spiny neurons from TAT2B and TAT2B(-SDV)-treated rats.

the last C-terminal three amino acids of the two subunits) was performed as control. In agreement with previous data (19), we found that both TAT2A and TAT2B induce a significant reduction of NMDA-evoked currents (TAT2A: *, $p < 0.05$, pre- *versus* post-TAT2A application, 64.03 ± 8.81% of control, $n = 4$; TAT2B: **, $p < 0.01$, pre- *versus* post-TAT2B application, 59.83 ± 2.62% of control, $n = 4$) (Fig. 2*A*). As expected (Fig. 2*B*; see Refs. 18 and 22), we observed a specific reduction of NR2A levels in the postsynaptic compartment following TAT2A treatment (**, $p < 0.01$, $n = 6$, NR2A, TAT2A *versus* control; Fig. 2*B*) and a specific reduction of NR2B levels following TAT2B application (**, $p < 0.01$, $n = 6$, NR2B, TAT2B *versus* control; Fig. 2*B*). Morphological analysis indicated no significant change in dendritic spine morphology after treatment with TAT2B ($p > 0.05$; Fig. 2*D*). Conversely, statistical analysis revealed a significant increase in spine head width after treatment with TAT2A (*, $p < 0.05$; TAT2A *versus* TAT2A(-SDV); Fig. 2*C*), confirming that reduction of NR2A- but not NR2B-containing NMDA receptor activity is *per se* sufficient to induce an enlargement of dendritic spine size.

*Localization of NMDA Receptor NR2A and NR2B Regulatory Subunits in D1- and D2-containing Striatal MSNs*—Previous reports performed in primary striatal cultures examined the modulation of NMDA receptor composition by D1 *versus* D2 dopamine receptors (29). However, no studies have been performed to clarify whether NR2A- and NR2B-containing NMDA receptors could show a distinct localization in the indirect and in the direct pathway MSNs. We used the drd1a-EGFP and drd2-EGFP BAC transgenic mice (30) that express EGFP under the control of either the D1 or D2 receptor promoters to assess the proportions of D1- and D2-positive MSNs expressing the NR2A subunit and those expressing the NR2B subunit of the NMDA receptor. To address this issue, we performed a double immunofluorescence analysis combining EGFP staining with NR2A and NR2B immunofluorescence in drd1a-EGFP (Fig. 3*A*) or drd2-EGFP (Fig. 3*B*) transgenic mice. Immunoflu-

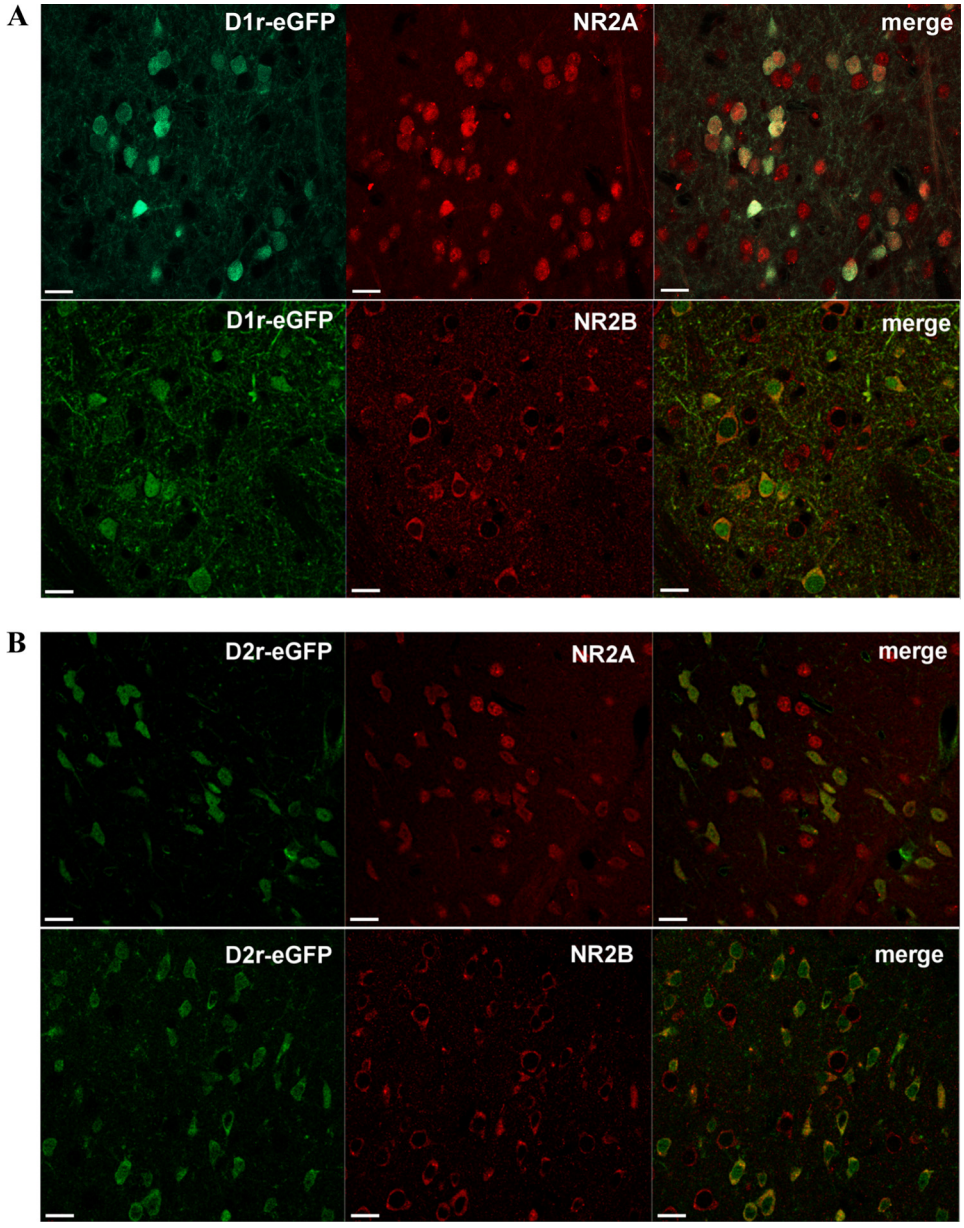


FIGURE 3. **Localization of NMDA receptor NR2A and NR2B regulatory subunits in D1- and D2-positive striatal MSNs.** Immunofluorescence analysis for NR2A (*upper panels*) and NR2B (*lower panels*) subunits of NMDA receptor in drd1a-EGFP (*A*) or drd2-EGFP (*B*) transgenic mice. Confocal analysis shows a complete overlap between NR2A and NR2B subunits and the two types of dopamine receptors in the transgenic mice, indicating the presence of the two NMDA regulatory subunits in all D1 and D2 containing MSNs. *Scale bar*, 30 $\mu$m.

orescent investigations revealed the presence of the two NMDA receptor regulatory subunits in all D1-positive as well as in all D2-positive striatal MSNs. In addition, we found a comparable colocalization degree of NR2B and NR2A with D1-positive (D1-EGFP/NR2A 51.4 ± 1.3%, neurons; D1-EGFP/NR2B 48.3 ± 1.5%; $n = 410$ neurons) and D2-positive neurons (D2-EGFP/NR2A 48.4 ± 1.1%, neurons; D2-EGFP/NR2B 50.6 ± 1.9%; $n = 290$ neurons).

*Influence of D1 Receptor Activation on NMDA Receptor Complex Composition at Postsynaptic Membrane*—Some reports indicate that activation of the D1-mediated signaling modulates NMDA receptor trafficking at synaptic sites (17, 29, 31, 32). Interestingly, corticostriatal long term potentiation is dependent on the activation of NMDA receptors, and it is blocked by D1 receptor antagonists or in mice lacking the D1 receptor (33). To assess the effect of D1 receptor activation on expression and synaptic localization of NR2A and NR2B NMDA subunits in striatum, we treated corticostriatal slices with the specific D1 receptor agonist SKF38393 (10 $\mu$M). Western blotting analysis performed in a post-synaptic TIF revealed that treatment with D1 agonist SKF38393 resulted in a significant change in the composition of the synaptic NMDA receptor, triggered by a significant decrease of NR2A subunit levels (***, $p < 0.001$, $n = 6$, NR2A, SKF38393 *versus* control; Fig. 4*A*), whereas NR2B remained unchanged ($p = 0.431$, $n = 6$, NR2B, SKF38393 *versus* control; Fig. 4*A*). No modification of NMDA receptor subunit levels was detected by Western blotting performed in the homogenate fraction after SKF38393 treatment (Fig. 4*A*). No significant modification of NR1 levels in the TIF was observed after treatment with D1 receptor agonist (data

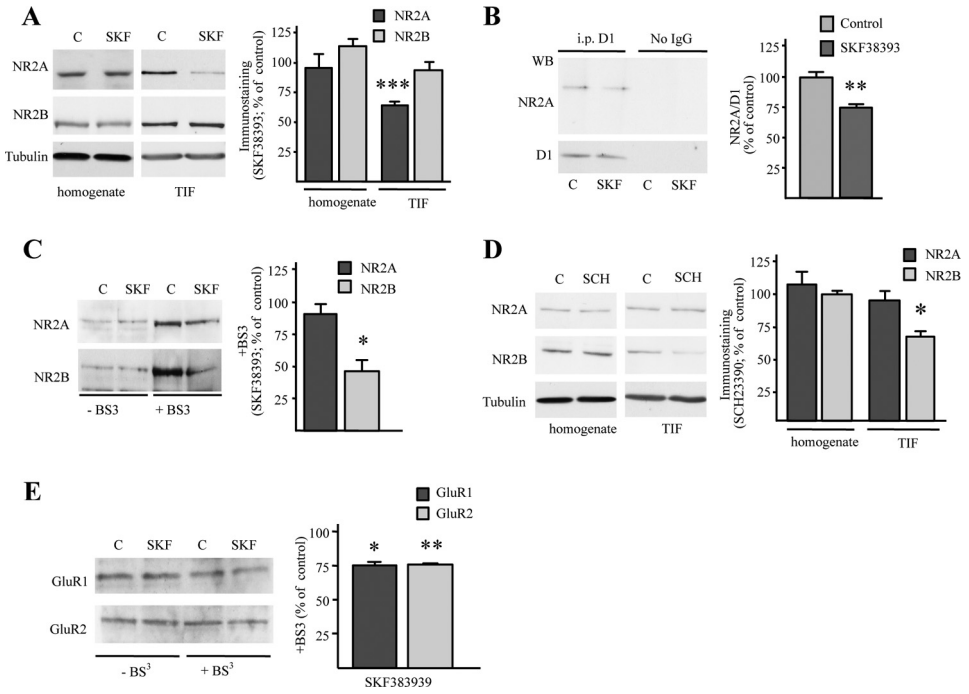


FIGURE 4. **D1 receptor modulation modifies NR2A/NR2B ratio in corticostriatal slices.** *A*, Western blot (*WB*) analysis of NR2A and NR2B subunits from the striatal homogenate and TIF fraction obtained from control (*C*) and SKF38393-treated (10 $\mu$M, 45 min) corticostriatal slices. The same amount of protein was loaded in each lane. The bar graph shows the amount of NR2A and NR2B subunits in the homogenate and TIF fraction from SKF38393-treated slices (*t* test; ***, $p < 0.001$). *B*, total homogenate was immunoprecipitated (i.p.) with antibody against D1 receptor and the presence of D1 and NR2A in the immunocomplex was evaluated by Western blot. Treatment with SKF38393 reduces NR2A co-precipitation with D1 (*t* test; **$p < 0.005$). *C*, Western blot of NR2A and NR2B subunits from control and SKF38393-treated corticostriatal slices exposed (+$BS^3$ lanes) or not (−$BS^3$ lanes) to the cross-linking agent $BS^3$. NMDA receptor subunits high-molecular weight complexes that did not enter the gel are not shown (*t* test; *, $p < 0.05$, NR2B, SKF38393 *versus* control). *D*, Western blot analysis of NR2A and NR2B subunits from the homogenate and TIF fraction obtained from control and SCH23390-treated (*SCH*, 45 min) corticostriatal slices. The same amount of proteins was loaded in each lane (*t* test; *, $p < 0.05$). *E*, Western blot of GluR1 and GluR2 subunits from control and SKF38393-treated corticostriatal slices exposed (+$BS^3$ lanes) or not (−$BS^3$ lanes) to the cross-linking agent $BS^3$. AMPA receptor subunits high-molecular weight complexes that did not enter the gel are not shown (*t* test; *, $p < 0.05$, GluR1, SKF38393 *versus* control; *t* test, **, $p < 0.01$, GluR2, SKF38393 *versus* control).

not shown). Co-immunoprecipitation of D1 receptor and NR2A subunit was performed after treatment of corticostriatal slice preparations with SKF38393. As shown previously (34), D1 receptor agonist produces a significant reduction of NR2A/D1 interaction (**, $p < 0.005$, $n = 4$, SKF38393 *versus* control; Fig. 4*B*).

Interestingly, analysis of the intracellular pool of NR2A and NR2B subunits by application of a membrane-impermeable cross-linker ($BS^3$) immediately after SKF38393 treatment, revealed no modification of NR2A subunit intracellular pool ($p = 0.359$, $n = 5$, NR2A, SKF38393 *versus* control; Fig. 4*C*). Conversely, treatment with SKF38393 reduced NR2B intracellular level (Fig. 4*C*) compared with control (*, $p < 0.05$, $n = 5$, NR2B, SKF38393 *versus* control), indicating an increased insertion of this subunit within the plasma membrane. In addition, treatment with SCH23390 (10 $\mu$M), a specific D1 receptor antagonist, induced a reduction of NR2B but not NR2A subunit in the postsynaptic fraction (TIF; *, $p < 0.05$, $n = 5$, NR2B, SCH23390 *versus* control, Fig. 4*D*), suggesting that D1 receptor antagonist produces a decrease of NR2B-containing NMDA receptors at synaptic membranes. Overall, these results indicate that D1 receptor activation produces a rearrangement of NMDA receptor composition, with a decrease of NR2A-containing NMDA receptors in the postsynaptic compartment.

*Influence of Dopamine Receptor Activation on AMPA Receptor Insertion within Plasma Membrane*—It has been shown previously that AMPA receptor cell surface expression can be up-regulated following D1 receptor activation (31, 35). We treated corticostriatal slices with the specific D1 receptor agonist SKF38393 and assessed the effect on membrane localization of GluR1 and GluR2 AMPA receptor subunits by using $BS^3$ cross-linking assay (Fig. 4*E*). Treatment with SKF38393 markedly decreased the intracellular pool of both GluR1 and GluR2 subunits compared with control slices indicating an increased insertion of the two subunits within the plasma membrane (*, $p < 0.05$, $n = 5$, GluR1, SKF38393 *versus* control; **, $p < 0.01$, $n = 5$, GluR2, SKF38393 *versus* control; Fig. 4*E*). No alteration of GluR1 and GluR2 localization in the triton insoluble synaptic fraction was observed after SKF38393 treatment (data not shown), suggesting that the modification of AMPA receptor subunits insertion in the membrane fraction observed after D1 receptor stimulation may be ascribed to a local trafficking within the synaptic compartment.

*Effect of Sustained Treatment with D1 Agonist on NMDA and AMPA Currents*—We then assessed the effect of long term D1 receptor stimulation on the NMDA receptor-AMPA receptor (NMDAR/AMPAR) ratio in MSNs by an electrophysiological characterization using patch clamp recordings. As shown in Fig. 5*A*, AMPA currents were evoked at −70 mV (inward currents), whereas NMDA currents were evoked at +40 mV (outward currents). Neurons were recorded 45 min after treatment with SKF38393 (10 $\mu$M) in corticostriatal slices. Interestingly, in 9 of 10 cells recorded, NMDAR/AMPAR ratios obtained were significantly reduced compared with the control experiments

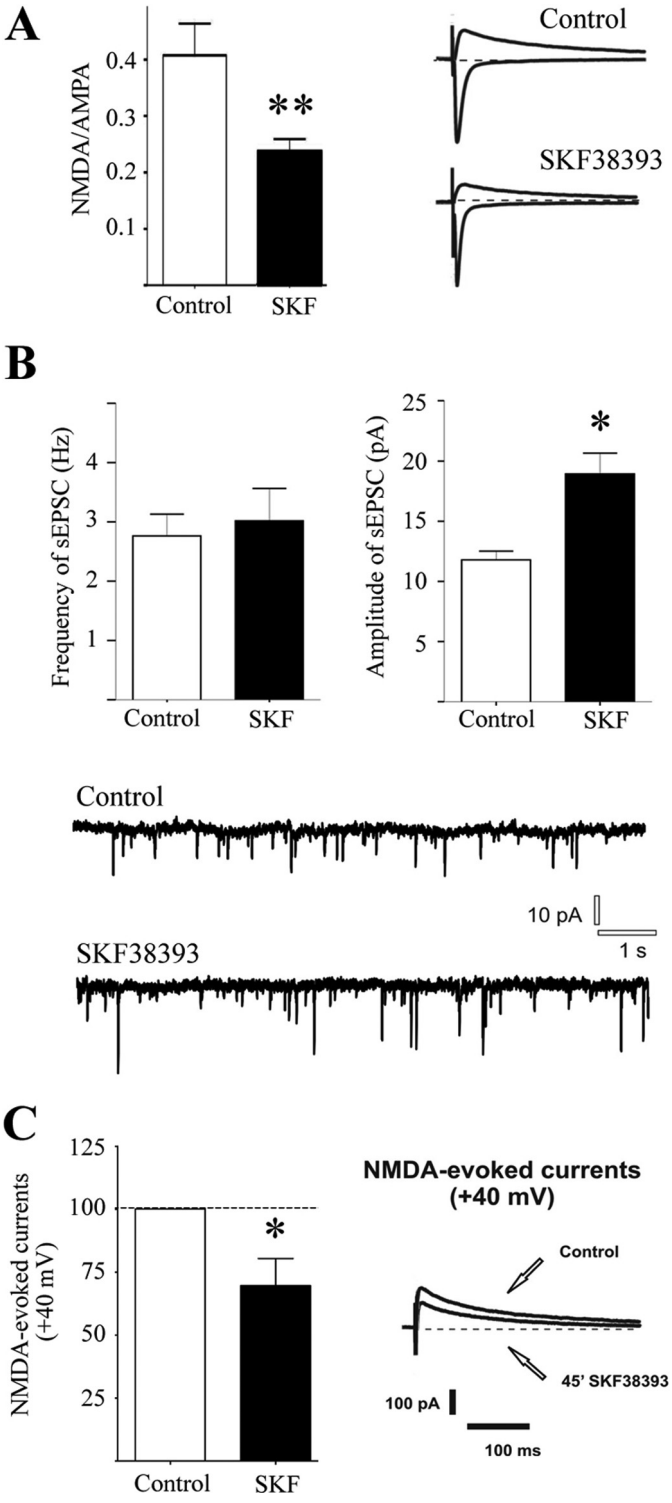


FIGURE 5. **Effect of sustained treatment with D1 agonist on NMDA and AMPA currents.** *A*, the bar graph on the *left panel* shows the effect of 45-min *in vitro* application of SKF38393 on the NMDAR/AMPAR ratio compared with control condition (**, $p < 0.01$; control, 0.41 ± 0.056; SKF38393, 0.23 ± 0.026; for each group, $n = 10$). In the *right panel* are reported averaged traces of AMPA currents (−70 mV in the presence of picrotoxin) and NMDA-evoked currents (+40 mV, in the presence of picrotoxin and CNQX) in control condition (*upper panel*) and after *in vitro* application of SKF38393 (*lower panel*). *B*, AMPA-mediated spontaneous excitatory activity. In the bar graphs are reported, respectively, the averaged values of the frequency (*left panel*) and amplitude (*right panel*) of spontaneous events AMPA-mediated recorded in MSNs from control slices and after 45 min of SKF38393 application. Representative traces from whole-cell patch clamp experiments showing glutamatergic AMPA-mediated spontaneous EPSCs from MSNs in control condition (*upper trace*) and in SKF-treated slice (*lower trace*). *C*, bar graph showing the effect of SKF incubation on the isolated NMDA-evoked current at +40 mV.

(**, $p < 0.01$, control 0.41 ± 0.056 *versus* SKF38393 0.23 ± 0.026; $n = 10$ for each group). All of the neurons recorded were simultaneously filled with biocytin through the recording pipette, and the following immunostaining revealed that the neurons were either positive for substance P ($SP^+$) or co-localized SP and A2A receptor ($SP^+/A2A^+$). Interestingly, the only cell in which no effect of SKF38393 was detected was found to be A2A-positive ($A2A^+$) (data not shown). To check whether the decrease in the NMDAR/AMPAR ratio observed was dependent on AMPAR or NMDAR modifications or both conditions, neurons were clamped at −70 mV, the AMPAR-mediated currents were isolated, and analysis of spontaneous activity performed. The amplitude of the spontaneous excitatory post-synaptic currents recorded in MSNs after 45 min of SKF38393 bath-applied was found to be increased significantly, suggesting an augmented activity of post-synaptic AMPAR (Fig. 5*B* (*, $p < 0.05$; control, 11.79 pA ± 0.32; 45 min of SKF38393, 18.94 pA ± 0.76; $n = 5$ for each group)). However, no significant changes were observed in terms of frequency of spontaneous EPSCs as shown in Fig. 5*B* (*left panel*; $p > 0.05$; control, 2.76 Hz ± 0.16; 45 min of SKF38393, 3.0176 ± 0.244; $n = 5$ for each group). To reveal a possible involvement of NMDAR in the change of NMDAR/AMPAR ratio, we moved to a different analysis because NMDAR-mediated spontaneous events were almost undetectable at −70 mV, even in the absence of magnesium ions in the extracellular solution. Therefore, we analyzed the effect of 45 min of SKF38393 bath-applied on the NMDAR-evoked currents obtained by clamping MSNs at +40 mV (Fig. 5*C*). Notably, this treatment reduced the current developed through the NMDAR when compared with control conditions, before drug application (*, $p < 0.05$; control *versus* 45 min of SKF38393, −30.34% ± 10.79%; $n = 3$).

*In Vivo Treatment with D1 Receptor Agonist SKF38393*—We then moved to *ex vivo* analysis, challenging the hypothesis that administration of the D1 receptor agonist SKF38393 *in vivo* could exert similar effects observed in *in vitro* system. In these series of experiments, rats were treated with the D1 receptor agonist (2 mg/ml/kg, i.p.; 45 min), and then biochemical and morphological experiments as well as recordings of corticostriatal slices were performed. *In vivo* treatment with D1 agonist SKF38393 resulted in a significant decrease in the synaptic level of the NR2A subunit (*, $p < 0.05$, $n = 5$, NR2A, SKF38393 *versus* control; Fig. 6*A*), whereas the NR2B subunit remained unchanged ($p = 0.711$, $n = 5$, NR2B, SKF38393 *versus* control; Fig. 6*A*), confirming the above-described results (see Fig. 4*A*) obtained by using acute corticostriatal slices preparations.

Interestingly, treatment with SKF38393 *in vivo* as *in vitro*, significantly reduced NMDAR/AMPAR ratio in 9 of 10 MSNs recorded when compared with control MSNs (**, $p < 0.01$, control 0.424 ± 0.188 *versus* SKF38393 0.16 ± 0.066; for each group $n = 10$) (Fig. 6*B*). Also under this condition, the lack of effect was parallel to the absence of SP fluorescence (data not shown). To confirm that the reduction of the ratio was dependent on the decrease in NR2A subunit, as demonstrated by

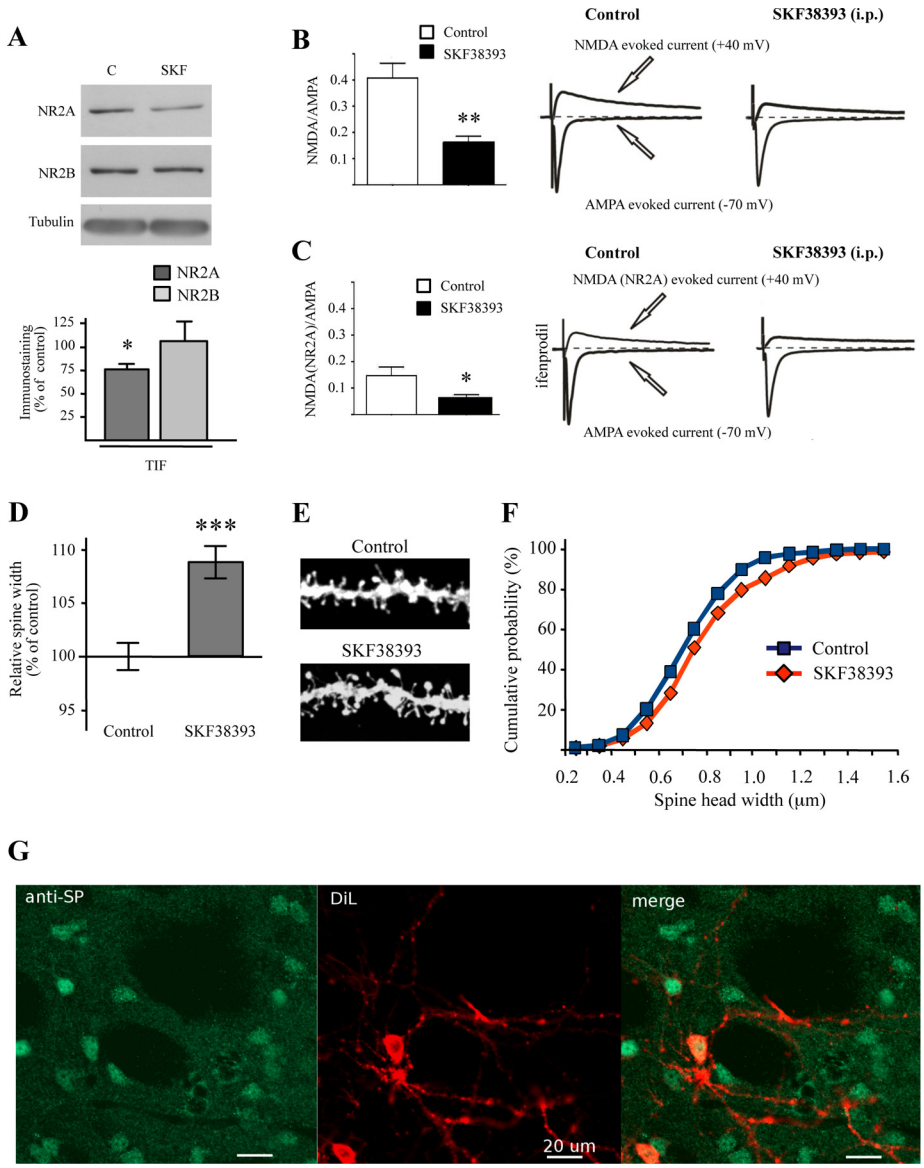


FIGURE 6. ***In vivo* treatment with D1 receptor agonist SKF38393.** *A*, Western blot analysis of NR2A and NR2B subunits performed in TIF fraction obtained from striatum of control and SKF38393-treated rats (2 mg/ml/kg, 45 min). The same amount of proteins was loaded in each lane (*t* test; *, $p < 0.05$). *B*, the bar graph on the *left panel* shows the effect of *in vivo* administration of SKF38393 (2 mg/ml/kg) on the NMDA-AMPA ratio compared with the control condition (**, $p < 0.01$; control, $0.424 \pm 0.188$; SKF38393, $0.16 \pm 0.066$; for each group, $n = 10$). In the *right panel* are reported averaged traces of AMPA currents (−70 mV in the presence of picrotoxin) and NMDA-evoked current (+40 mV, in the presence of picrotoxin and CNQX) in control condition (*left side*) and after *in vivo* administration of 2 mg/ml/kg SKF (*right side*). *C*, the bar graph on the *left panel* shows the effect of *in vivo* administration of SKF38393 on the NMDA(NR2A)-AMPA ratio. In the *right panel* are presented averaged traces of AMPA currents and NMDA(NR2A) currents (+40 mV in the presence of picrotoxin, CNQX, and ifenprodil) in control condition (*left side*) and after *in vivo* administration of SKF (*right side*) (*, $p < 0.05$; control, $0.146 \pm 0.086$; SKF38393, $0.063 \pm 0.03$, respectively, $n = 7$ and $n = 6$). *D*, diagram showing relative average spines head width (*t* test; $n > 380$ spines from nine different neurons for each group; ***, $p < 0.0001$ SKF38393 *versus* control). *F*, cumulative frequency plots of spine head width of MSNs from control (*blue*) or SKF38393-treated (*red*) rats. *E*, representative images show dendrites of MSNs from control or SKF38393-treated rats. *G*, immunohistochemistry showing colocalization of SP-positive neurons (anti-SP, *green*) and diolistic labeling (*DiL*, *red*).

biochemical data, 10 $\mu$M ifenprodil (20) was applied on the NMDA-EPSC component to disclose the NR2A component. Importantly, the pharmacological isolation of NR2A subunit revealed that the NMDA(NR2A)-AMPA ratio was significantly reduced by the pharmacological treatment with SKF38393 (*, $p < 0.05$, control $0.146 \pm 0.086$ *versus* SKF38393 $0.063 \pm 0.03$; $n = 7$ and $n = 6$, respectively) (Fig. 6*C*). Similar data were obtained after application of 3 $\mu$M ifenprodil (data not shown).

The above-described experiments show that D1 receptor activation leads to a modification of NR2A/NR2B containing NMDA receptors at synaptic sites and to a concomitant increase of AMPA receptor amount within the membrane fraction. Immunohistochemistry combined with diolistic labeling was performed to evaluate average spine head width of dendritic spines selectively in substance P-positive ($SP^+$; direct pathway) MSNs (Fig. 6*G*). Statistical analysis revealed a significant increase in spine head width after treatment with SKF38393 (Fig. 6, *D* and *E*; ***, $p < 0.0001$, spine width, SKF38393 *versus* control) and cumulative frequency plots of spine head width confirmed a shift toward bigger spine size (Fig. 6*F*).

*NR2A and NR2B Antagonists Differentially Modulate D1-dependent Effect on Dendritic Spine Morphology*—We repeated morphological analysis in corticostriatal slices after *in vivo*

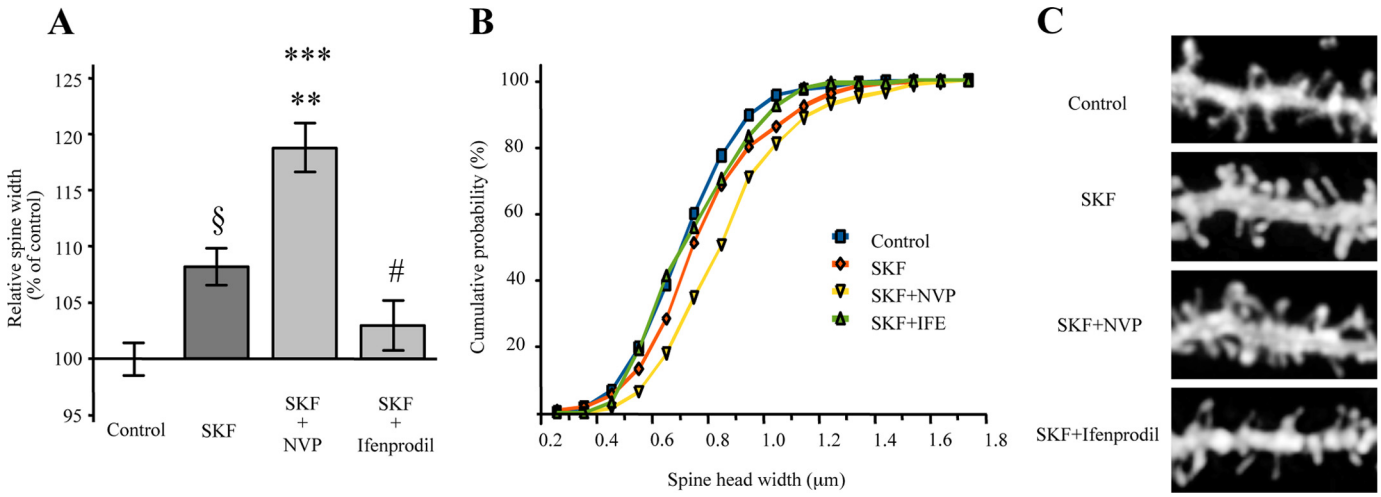


FIGURE 7. **Effect of the selective NR2A and NR2B antagonists on D1-mediated modification of dendritic spine morphology.** *A*, diagram showing relative average spine head widths (Kruskal-Wallis non-parametric analysis of variance; §, $p < 0.0005$; SKF38393 (*SKF*) *versus* control; ***, $p < 0.0001$; SKF38393+NVP-AAM077 *versus* control; **, $p < 0.01$; SKF38393+NVP-AAM077 *versus* SKF38393; #, $p < 0.005$ SKF38393+ifenprodil *versus* SKF38393; $n > 320$ spines from eight different neurons for each group). *B*, cumulative frequency plots of spine head width of medium spiny neurons from control, SKF38393, SKF38393+NVP-AAM077 (*NVP*), or SKF38393+ifenprodil-treated (*IFP*) rats. *C*, representative images show dendrites of medium spiny neurons from control or treated rats.

treatment with SKF38393 in presence or absence of NR2A (NVP-AAM077) or NR2B (ifenprodil)-specific antagonists to evaluate whether the effects of D1 receptor activation on spine size are dependent on the observed modulation in NR2B/NR2A ratio at synaptic sites (see Figs. 4–6). As indicated also above, morphological analysis was performed in SP-positive neurons (data not shown). Statistical analysis revealed a significant increase in spine head width (Fig. 7, *A–C*) after treatment with SKF38393 in the presence or absence of NVP-AAM077 (§, $p < 0.0005$, SKF38393 *versus* control; ***, $p < 0.0001$, SKF38393+NVP-AAM077 *versus* control). Notably, treatment with SKF38393+NVP-AAM077 induced a significant increase in spine head width also compared with SKF38393 alone (**, $p < 0.01$, SKF38393+NVP-AAM077 *versus* SKF38393). Conversely, statistical analysis revealed a significant decrease of spine head width in SKF38393+ifenprodil-treated rats compared with SKF38393 (#, $p < 0.005$, SKF38393+ifenprodil *versus* SKF38393). No significant modification of dendritic spine morphology was observed between control and SKF38393+ifenprodil-treated rats ($p > 0.05$, SKF38393+ifenprodil *versus* control). As described also above (see Fig. 1), treatment with NVP-AAM077 alone induced a significant increase in spine head width compared with control (*, $p < 0.05$, NVP-AAM077 *versus* control, data not shown). Conversely, no modification of spine morphology was observed between control and ifenprodil-treated rats ($p > 0.05$, ifenprodil *versus* control, data not shown).

No significant changes in the mean spine density were found (SKF38393, 8.31 ± 0.51 spines/10 μm; control, 9.21 ± 0.84 spines/10 μm; NVP-AAM077, 10.12 ± 0.46 spines/10 μm; ifenprodil, 9.27 ± 0.59 spines/10 μm; SKF38393+NVP-AAM077, 9.67 ± 0.39 spines/10 μm; SKF38393+ifenprodil, 8.90 ± 0.46 spines/10 μm). Overall, morphological analysis demonstrates that treatment with NR2A antagonist NVP-AAM077 significantly increases the effect on dendritic spine head width induced by the D1 agonist. Conversely, the NR2B antagonist ifenprodil blocks any morphological effect prompted by D1 activation.

## DISCUSSION

NMDA receptor subunit composition strictly commands receptor function and pharmacological responses (36). In striatum, activation of NR2A- or NR2B-containing NMDARs differentially modulate GABA and glutamate release in target areas within the basal ganglia (37) as well as glutamatergic synaptic transmission and evoked dopamine release within the striatum (16). However, the role of distinct NR2 subunits in dendritic spine remodeling as well as in the induction of plasticity events in the striatum has not yet been investigated. Here, we show that variation of the levels of NR2A-containing NMDA receptors at synaptic sites induces a significant modification of dendritic spine morphology in striatal MSNs. Treatment with NR2A antagonist or with NR2A blocking peptide induces a significant increase of spine head width in striatal MSNs. Notably, prolonged activation of D1 receptor, inducing a specific reduction of synaptic NR2A-containing NMDA receptors, leads to a similar morphological outcome.

Dendritic spines of MSNs are an essential site of information processing from glutamate and dopamine afferents in striatum both in physiological conditions and in neurodegenerative events, *i.e.* in PD (8). The size of dendritic spine heads reflects synaptic strength, thus indicating that a significant modification in spine head diameter influences neuronal plasticity. Previous studies, mainly performed in animal models for CNS diseases, suggested that dopamine plays an important role in regulating spine density on striatal MSNs (38). Day and colleagues (39) demonstrated that dopamine depletion causes a loss of dendritic spines selectively on indirect pathway neurons, suggesting a D2 receptor-mediated regulation of the L-type Cav1.3 channel in this morphological event. In contrast, recent studies put forward the existence of a D1-dependent signaling pathway regulating spine morphology at MSN levels (40–42).

Exposure to psychostimulants leads to increase dendritic spine density mainly in D1-containing MSNs (40). More recently, Ren and co-workers (42) proposed that D1 and NMDA receptors may cooperate to neuronal morphological changes induced by repeated exposure to cocaine. Here, we show that sustained D1 receptor activation obtained with a classical receptor agonist, SKF38393, determines a significant increase of dendritic spine head width and a concomitant rearrangement of NMDA receptor subunit composition due to a decrease of synaptic NR2A-containing receptors. Notably, treatment with NR2A antagonist NVP-AAM077 or with NR2A blocking peptide is sufficient to induce a significant morphological modification of dendritic spine head width comparable with that obtained with the D1 agonist.

Interestingly, our results also suggest that the observed reduction of the NR2A subunit in the postsynaptic compartment following treatment with SKF38393 could be ascribed to a movement of NR2A-containing NMDA receptors from synaptic to extrasynaptic membranes. In contrast, the reduction of NR2B intracellular pool together with no modification of NR2B levels in the triton-insoluble postsynaptic fraction suggests a local insertion of the NR2B-containing NMDA receptor in the postsynaptic membrane, in agreement with previous reports (15, 29).

Several studies have demonstrated a temporal and functional correlation between synaptic accumulation of AMPA receptors and dendritic spine growth (43, 44). Consistently, in our experiment, a prolonged treatment with D1 receptor agonist leads not only to a reduction of NR2A *versus* NR2B-containing NMDA receptors at synaptic sites but also to a concomitant increase of AMPA receptor subunits insertion in the postsynaptic membrane. These results confirm, at MSN levels, the existence of the above-indicated coordination among dendritic spine size and AMPA receptor content already demonstrated in the hippocampus (43, 44).

We recently observed an increased expression of synaptic NR2A subunits in a model of early PD (19) as well as in rat models of L-DOPA-induced dyskinesia (18, 28). In particular, we demonstrated that an unbalanced NR2A/NR2B subunit ratio of the synaptic NMDA receptor is a key element in the regulation of motor behavior and synaptic plasticity in the early stages of PD (8, 19). In addition, we demonstrated that targeting D1 receptors by systemic administration of SKF38393 normalizes NMDA receptor subunit composition and improves motor behavior in the model of early PD, establishing a critical link among a specific subgroup of dopamine/NMDA receptors and motor performances (19). The results presented here confirm these data demonstrating that a sustained D1 receptor activation induces a significant modification of NR2A/NR2B ratio at synaptic sites, providing a morphological/functional outcome at dendritic spine level associated to this molecular event.

## REFERENCES


1. Lüthi, A., Schwyzer, L., Mateos, J. M., Gähwiler, B. H., and McKinney, R. A. (2001) NMDA receptor activation limits the number of synaptic connections during hippocampal development. *Nat. Neurosci.* **4,** 1102–1107
2. Adesnik, H., Li, G., During, M. J., Pleasure, S. J., and Nicoll, R. A. (2008) NMDA receptors inhibit synapse unsilencing during brain development. *Proc. Natl. Acad. Sci. U.S.A.* **105,** 5597–5602
3. Lu, W., Man, H., Ju, W., Trimble, W. S., MacDonald, J. F., and Wang, Y. T. (2001) Activation of synaptic NMDA receptors induces membrane insertion of new AMPA receptors and LTP in cultured hippocampal neurons. *Neuron* **29,** 243–254
4. Merriam, E. B., Lumbard, D. C., Viesselmann, C., Ballweg, J., Stevenson, M., Pietila, L., Hu, X., and Dent, E. W. (2011) Dynamic microtubules promote synaptic NMDA receptor-dependent spine enlargement. *PLoS One* **6,** e27688
5. McKinney, R. A. (2010) Excitatory amino acid involvement in dendritic spine formation, maintenance, and remodeling. *J. Physiol.* **588,** 107–116
6. Fiala, J. C., Feinberg, M., Popov, V., and Harris, K. M. (1998) Synaptogenesis via dendritic filopodia in developing hippocampal area CA1. *J. Neurosci.* **18,** 8900–8911
7. Surmeier, D. J., Ding, J., Day, M., Wang, Z., and Shen, W. (2007) D1 and D2 dopamine-receptor modulation of striatal glutamatergic signaling in striatal medium spiny neurons. *Trends Neurosci.* **30,** 228–235
8. Gardoni, F., Ghiglieri, V., Luca, M., and Calabresi, P. (2010) Assemblies of glutamate receptor subunits with post-synaptic density proteins and their alterations in Parkinson disease. *Prog. Brain Res.* **183,** 169–182
9. Fiorentini, C., Gardoni, F., Spano, P., Di Luca, M., and Missale, C. (2003) Regulation of dopamine D1 receptor trafficking and desensitization by oligomerization with glutamate *N*-methyl-D-aspartate receptors. *J. Biol. Chem.* **278,** 20196–20202
10. Jocoy, E. L., André, V. M., Cummings, D. M., Rao, S. P., Wu, N., Ramsey, A. J., Caron, M. G., Cepeda, C., and Levine, M. S. (2011) Dissecting the contribution of individual receptor subunits to the enhancement of *N*-methyl-D-aspartate currents by dopamine D1 receptor activation in striatum. *Front. Syst. Neurosci.* **5,** 28
11. Kruusmägi, M., Kumar, S., Zelenin, S., Brismar, H., Aperia, A., and Scott, L. (2009) Functional differences between D1 and D5 revealed by high resolution imaging on live neurons. *Neuroscience* **164,** 463–469
12. Albers, D. S., Weiss, S. W., Iadarola, M. J., and Standaert, D. G. (1999) Immunohistochemical localization of *N*-methyl-D-aspartate and α-amino-3-hydroxy-5-methyl-4-isoxazolepropionate receptor subunits in the substantia nigra pars compacta of the rat. *Neuroscience* **89,** 209–220
13. Li, L., Murphy, T. H., Hayden, M. R., and Raymond, L. A. (2004) Enhanced striatal NR2B-containing *N*-methyl-D-aspartate receptor-mediated synaptic currents in a mouse model of Huntington disease. *J. Neurophysiol.* **92,** 2738–4276
14. Chapman, D. E., Keefe, K. A., and Wilcox, K. S. (2003) Evidence for functionally distinct synaptic NMDA receptors in ventromedial *versus* dorsolateral striatum. *J. Neurophysiol.* **89,** 69–80
15. Dunah, A. W., and Standaert, D. G. (2003) Subcellular segregation of distinct heteromeric NMDA glutamate receptors in the striatum. *J. Neurochem.* **85,** 935–943
16. Schotanus, S. M., and Chergui, K. (2008) NR2A-containing NMDA receptors depress glutamatergic synaptic transmission and evoked dopamine release in the mouse striatum. *J. Neurochem.* **106,** 1758–1765
17. Dunah, A. W., and Standaert, D. G. (2001) Dopamine D1 receptor-dependent trafficking of striatal NMDA glutamate receptors to the postsynaptic membrane. *J. Neurosci.* **21,** 5546–5558
18. Gardoni, F., Picconi, B., Ghiglieri, V., Polli, F., Bagetta, V., Bernardi, G., Cattabeni, F., Di Luca, M., and Calabresi, P. (2006) A critical interaction between NR2B and MAGUK in L-DOPA-induced dyskinesia. *J. Neurosci.* **26,** 2914–2922
19. Paillé, V., Picconi, B., Bagetta, V., Ghiglieri, V., Sgobio, C., Di Filippo, M., Viscomi, M. T., Giampà, C., Fusco, F. R., Gardoni, F., Bernardi, G., Greengard, P., Di Luca, M., and Calabresi, P. (2010) Distinct levels of dopamine denervation differentially alter striatal synaptic plasticity and NMDA receptor subunit composition. *J. Neurosci.* **30,** 14182–14193
20. Milnerwood, A. J., Gladding, C. M., Pouladi, M. A., Kaufman, A. M., Hines, R. M., Boyd, J. D., Ko, R. W., Vasuta, O. C., Graham, R. K., Hayden, M. R., Murphy, T. H., and Raymond, L. A. (2010) Early increase in extrasynaptic NMDA receptor signaling and expression contributes to phenotype onset in Huntington disease mice. *Neuron* **65,** 178–190
21. Aarts, M., Liu, Y., Liu, L., Besshoh, S., Arundine, M., Gurd, J. W., Wang, Y. T., Salter, M. W., and Tymianski, M. (2002) Treatment of ischemic

brain damage by perturbing NMDA receptor: PSD-95 protein interactions. *Science* **298,** 846–850
22. Gardoni, F., Mauceri, D., Malinverno, M., Polli, F., Costa, C., Tozzi, A., Siliquini, S., Picconi, B., Cattabeni, F., Calabresi, P., and Di Luca, M. (2009) Decreased NR2B subunit synaptic levels cause impaired long term potentiation but not long term depression. *J. Neurosci.* **29,** 669–677
23. Gardoni, F., Bellone, C., Cattabeni, F., and Di Luca, M. (2001) Protein kinase C activation modulates α-calmodulin kinase II binding to NR2A subunit of *N*-methyl-D-aspartate receptor complex. *J. Biol. Chem.* **276,** 7609–7613
24. Mauceri, D., Cattabeni, F., Di Luca, M., and Gardoni, F. (2004) Calcium/calmodulin-dependent protein kinase II phosphorylation drives synapse-associated protein 97 into spines. *J. Biol. Chem.* **279,** 23813–23821
25. Neely, M. D., Stanwood, G. D., and Deutch, A. Y. (2009) Combination of diOlistic labeling with retrograde tract tracing and immunohistochemistry. *J. Neurosci. Methods* **184,** 332–336
26. Bourne, J. N., and Harris, K. M. (2008) Balancing structure and function at hippocampal dendritic spines. *Annu. Rev. Neurosci.* **31,** 47–67
27. Lau, C. G., and Zukin, R. S. (2007) NMDA receptor trafficking in synaptic plasticity and neuropsychiatric disorders. *Nat. Rev. Neurosci.* **8,** 413–426
28. Gardoni, F., Sgobio, C., Pendolino, V., Calabresi, P., Di Luca, M., and Picconi, B. (2011) Targeting NR2A-containing NMDA receptors reduces L-DOPA-induced dyskinesias. *Neurobiol. Aging* [Epub ahead of print]
29. Hallett, P. J., Spoelgen, R., Hyman, B. T., Standaert, D. G., and Dunah, A. W. (2006) Dopamine D1 activation potentiates striatal NMDA receptors by tyrosine phosphorylation-dependent subunit trafficking. *J. Neurosci.* **26,** 4690–4700
30. Valjent, E., Bertran-Gonzalez, J., Hervé, D., Fisone, G., and Girault, J. A. (2009) Looking BAC at striatal signaling: cell-specific analysis in new transgenic mice. *Trends Neurosci.* **32,** 538–547
31. Price, C. J., Kim, P., and Raymond, L. A. (1999) D1 dopamine receptor-induced cyclic AMP-dependent protein kinase phosphorylation and potentiation of striatal glutamate receptors. *J. Neurochem.* **73,** 2441–2446
32. Dunah, A. W., Sirianni, A. C., Fienberg, A. A., Bastia, E., Schwarzschild, M. A., and Standaert, D. G. (2004) Dopamine D1-dependent trafficking of striatal *N*-methyl-D-aspartate glutamate receptors requires Fyn protein tyrosine kinase but not DARPP-32. *Mol. Pharmacol.* **65,** 121–129
33. Di Filippo, M., Picconi, B., Tantucci, M., Ghiglieri, V., Bagetta, V., Sgobio, C., Tozzi, A., Parnetti, L., and Calabresi, P. (2009) Short term and long term plasticity at corticostriatal synapses: Implications for learning and memory. *Behav. Brain Res.* **199,** 108–118
34. Lee, F. J., Xue, S., Pei, L., Vukusic, B., Chéry, N., Wang, Y., Wang, Y. T., Niznik, H. B., Yu, X. M., and Liu, F. (2002) Dual regulation of NMDA receptor functions by direct protein-protein interactions with the dopamine D1 receptor. *Cell* **111,** 219–230
35. Mangiavacchi, S., and Wolf, M. E. (2004) D1 dopamine receptor stimulation increases the rate of AMPA receptor insertion onto the surface of cultured nucleus accumbens neurons through a pathway dependent on protein kinase A. *J. Neurochem.* **88,** 1261–1271
36. Paoletti, P., and Neyton, J. (2007) NMDA receptor subunits: Function and pharmacology. *Curr. Opin. Pharmacol.* **7,** 39–47
37. Fantin, M., Marti, M., Auberson, Y. P., and Morari, M. (2007) NR2A and NR2B subunit containing NMDA receptors differentially regulate striatal output pathways. *J. Neurochem.* **103,** 2200–2211
38. Arbuthnott, G. W., Ingham, C. A., and Wickens, J. R. (2000) Dopamine and synaptic plasticity in the neostriatum. *J. Anat.* **196,** 587–596
39. Day, M., Wang, Z., Ding, J., An, X., Ingham, C. A., Shering, A. F., Wokosin, D., Ilijic, E., Sun, Z., Sampson, A. R., Mugnaini, E., Deutch, A. Y., Sesack, S. R., Arbuthnott, G. W., and Surmeier, D. J. (2006) Selective elimination of glutamatergic synapses on striatopallidal neurons in Parkinson disease models. *Nat. Neurosci.* **9,** 251–259
40. Lee, K. W., Kim, Y., Kim, A. M., Helmin, K., Nairn, A. C., and Greengard, P. (2006) Cocaine-induced dendritic spine formation in D1 and D2 dopamine receptor-containing medium spiny neurons in nucleus accumbens. *Proc. Natl. Acad. Sci. U.S.A.* **103,** 3399–3404
41. McAvoy, T., Zhou, M. M., Greengard, P., and Nairn, A. C. (2009) Phosphorylation of Rap1GAP, a striatally enriched protein, by protein kinase A controls Rap1 activity and dendritic spine morphology. *Proc. Natl. Acad. Sci. U.S.A.* **106,** 3531–3536
42. Ren, Z., Sun, W. L., Jiao, H., Zhang, D., Kong, H., Wang, X., and Xu, M. (2010) Dopamine D1 and *N*-methyl-D-aspartate receptors and extracellular signal-regulated kinase mediate neuronal morphological changes induced by repeated cocaine administration. *Neuroscience* **168,** 48–60
43. Kasai, H., Matsuzaki, M., Noguchi, J., Yasumatsu, N., and Nakahara, H. (2003) Structure-stability-function relationships of dendritic spines. *Trends Neurosci.* **26,** 360–368
44. Kopec, C. D., Real, E., Kessels, H. W., and Malinow, R. (2007) GluR1 links structural and functional plasticity at excitatory synapses. *J. Neurosci.* **27,** 13706–13718